VOLUME 35 | SUPPLEMENT 2 | MARCH 2022

MODERN PATHOLOGY

ABSTRACTS (356–371)

ENDOCRINE PATHOLOGY

2022

USCAP 111TH ANNUAL MEETING

REAL INTELLIGENCE

MARCH 19–24, 2022 LOS ANGELES, CALIFORNIA

Published by
SPRINGER NATURE
www.ModernPathology.org

USCAP Creating a Better Pathologist
AN OFFICIAL JOURNAL OF THE UNITED STATES AND CANADIAN ACADEMY OF PATHOLOGY

EDUCATION COMMITTEE

Rhonda K. Yantiss
Chair

Kristin C. Jensen
Chair, CME Subcommittee

Laura C. Collins
Chair, Interactive Microscopy Subcommittee

Yuri Fedoriw
Short Course Coordinator

Ilan Weinreb
Chair, Subcommittee for Unique Live Course Offerings

Carla L. Ellis
Chair, DEI Subcommittee

Adebowale J. Adeniran
Kimberly H. Allison
Sarah M. Dry
William C. Faquin
Karen J. Fritchie
Jennifer B. Gordetsky
Levon Katsakhyan, Pathologist-in-Training
Melinda J. Lerwill
M. Beatriz S. Lopes
Julia R. Naso, Pathologist-in-Training
Liron Pantanowitz
Carlos Parra-Herran
Rajiv M. Patel
Charles "Matt" Quick
David F. Schaeffer
Lynette M. Sholl
Olga K. Weinberg
Maria Westerhoff

ABSTRACT REVIEW BOARD

Benjamin Adam
Oyedele Adeyi
Mariam Priya Alexander
Daniela Allende
Catalina Amador
Vijayalakshmi Ananthanarayanan
Tatjana Antic
Manju Aron
Roberto Barrios
Gregory R. Bean
Govind Bhagat
Luis Zabala Blanco
Michael Bonert
Alain C. Borczuk
Tamar C. Brandler
Eric Jason Burks
Kelly J. Butnor
Sarah M. Calkins
Weibiao Cao
Wenqing (Wendy) Cao
Barbara Ann Centeno
Joanna SY Chan
Kung-Chao Chang
Hao Chen
Wei Chen
Yunn-Yi Chen
Sarah Chiang
Soo-Jin Cho
Shefali Chopra
Nicole A. Cipriani
Cecilia Clement
Claudiu Cotta
Jennifer A. Cotter
Sonika M. Dahiya
Elizabeth G. Demicco
Katie Dennis
Jasreman Dhillon
Anand S. Dighe
Bojana Djordjevic
Michelle R. Downes
Charles G. Eberhart
Andrew G. Evans
Fang Fan
Julie C. Fanburg-Smith
Gelareh Farshid
Michael Feely
Susan A. Fineberg
Dennis J. Firchau
Gregory A. Fishbein
Agnes B. Fogo
Andrew L. Folpe
Danielle Fortuna
Billie Fyfe-Kirschner
Zeina Ghorab
Giovanna A. Giannico
Anthony J. Gill
Tamar A. Giorgadze
Alessio Giubellino
Carolyn Glass
Carmen R. Gomez-Fernandez
Shunyou Gong
Purva Gopal
Abha Goyal
Christopher C. Griffith
Ian S. Hagemann
Gillian Leigh Hale
Suntrea TG Hammer
Malini Harigopal
Kammi J. Henriksen
Jonas J. Heymann
Carlo Vincent Hojilla
Aaron R. Huber
Jabed Iqbal
Shilpa Jain
Vickie Y. Jo
Ivy John
Dan Jones
Ridas Juskevicius
Meghan E. Kapp
Nora Katabi
Francesca Khani
Joseph D. Khoury
Benjamin Kipp
Veronica E. Klepeis
Christian A. Kunder
Stefano La Rosa
Stephen M. Lagana
Keith K. Lai
Goo Lee
Michael Lee
Vasiliki Leventaki
Madelyn Lew
Faqian Li
Ying Li
Chieh-Yu Lin
Mikhail Lisovsky
Lesley C. Lomo
Fang-I Lu
aDeqin Ma
Varsha Manucha
Rachel Angelica Mariani
Brock Aaron Martin
David S. McClintock
Anne M. Mills
Richard N. Mitchell
Hiroshi Miyamoto
Kristen E. Muller
Priya Nagarajan
Navneet Narula
Michiya Nishino
Maura O'Neil
Scott Roland Owens
Burcin Pehlivanoglu
Deniz Peker Barclift
Avani Anil Pendse
Andre Pinto
Susan Prendeville
Carlos N. Prieto Granada
Peter Pytel
Stephen S. Raab
Emilian V. Racila
Stanley J. Radio
Santiago Ramon Y Cajal
Kaaren K Reichard
Jordan P. Reynolds
Lisa M. Rooper
Andrew Eric Rosenberg
Ozlen Saglam
Ankur R. Sangoi
Kurt B. Schaberg
Qiuying (Judy) Shi
Wonwoo Shon
Pratibha S. Shukla
Gabriel Sica
Alexa Siddon
Anthony Sisk
Kalliopi P. Siziopikou
Stephanie Lynn Skala
Maxwell L. Smith
Isaac H. Solomon
Wei Song
Simona Stolnicu
Adrian Suarez
Paul E. Swanson
Benjamin Jack Swanson
Sara Szabo
Gary H. Tozbikian
Gulisa Turashvili
Andrew T. Turk
Efsevia Vakiani
Paul VanderLaan
Hanlin L. Wang
Stephen C. Ward
Kevin M. Waters
Jaclyn C. Watkins
Shi Wei
Hannah Y. Wen
Kwun Wah Wen
Kristy Wolniak
Deyin Xing
Ya Xu
Shaofeng N. Yan
Zhaohai Yang
Yunshin Albert Yeh
Huina Zhang
Xuchen Zhang
Bihong Zhao
Lei Zhao

To cite abstracts in this publication, please use the following format: **Author A, Author B, Author C, et al. Abstract title (abs#). In "File Title."** ***Modern Pathology*** **2022; 35 (suppl 2): page#**

356 BRAF-TERT Signature and PD-L1 Expression in Radioiodine-Refractory Locoregional Recurrences of Papillary Thyroid Carcinoma

Andrey Bychkov[1], Usanee Techavijit[2], Chan Kwon Jung[3], Somboon Keelawat[2], Supatporn Tepmongkol[2]
[1]Kameda Medical Center, Kamogawa, Japan, [2]Chulalongkorn University, Bangkok, Thailand, [3]The Catholic University of Korea, Seoul St. Mary's Hospital, Seoul, South Korea

Disclosures: Andrey Bychkov: None; Usanee Techavijit: None; Chan Kwon Jung: None; Somboon Keelawat: None; Supatporn Tepmongkol: None

Background: Despite an excellent long-term prognosis, up to 20% of patients with papillary thyroid carcinoma (PTC) experience regional or distant recurrence. About one third of these recurrences become radioiodine-refractory (RAIR), which significantly worsens prognosis. BRAF V600E and TERT promoter mutations were recently identified as predictors of RAIR in distant metastases of PTC. Locoregionally recurrent PTCs are not infrequent, however there is a lack of knowledge about molecular events in these lesions due to rarity of sampling. We aimed to study histopathological characteristics, PD-L1 expression, BRAF-TERT signature, and clinical correlates in RAIR cervical recurrences of PTC.

Design: A total of 66 cases (mean age – 56.1, sex ratio – 0.37) were qualified as eligible from a cohort of 1857 patients with PTC who received post-thyroidectomy RAI ablation. Locoregional recurrence was defined as a histopathologically confirmed tumor recurrence within the neck. A case was considered RAIR if the patient had an elevated serum thyroglobulin (>10 ng/ml) under a high thyrotropin level with structural disease in the setting of a negative RAI scan, or disease progressed after receiving more than 600 mCi of RAI. We performed pyrosequencing for BRAF V600E and TERT promoter C228T and C250T mutations. PD-L1 expression was evaluated with Ventana SP263 clone.

Results: Histologically, most of the cervical recurrences were of lymph node origin, with frequent extranodal extension. Predominant patterns were papillary, tall cell, and solid. TERT promoter mutations were found in 28/65 (43%) cases, including 23 cases with TERT C228T and 5 cases with TERT C250T. BRAF V600E mutation was found in 52/66 (78.8%) cases. Coexistence of TERT promoter and BRAF mutations was found in 25/66 (37.9%) recurrent PTCs, while 11/66 (16.7%) cases were BRAF-/TERT-. PD-L1 expression (> 1%) was detected in 21/36 cases available for evaluation, including 10/36 cases with immunoexpression in over 25% cancer cells. On a mean follow-up of 63.5 months, 18/66 (27.3%) patients died of disease. TERT promoter mutation and BRAF/TERT combination were found less frequently in surviving patients; however only BRAF/TERT co-mutation was statistically associated with a death by disease ($p = 0.04$).

Conclusions: This is the first study describing the high prevalence of BRAF and TERT promoter mutations in a carefully selected cohort of RAIR locoregional recurrences of PTC. RAIR tumors showed frequent PD-L1 expression, which may have clinical implications.

357 RET Splice Site Variants in Medullary Thyroid Carcinoma

Kyriakos Chatzopoulos[1], Daryoush Saeed-Vafa[2], Juan Hernandez-Prera[2], Pedro Cano[2], James Saller[2], Bryan McIver[2], Theresa Boyle[2]
[1]Mayo Clinic, Rochester, MN, [2]H. Lee Moffitt Cancer Center & Research Institute, Tampa, FL

Disclosures: Kyriakos Chatzopoulos: None; Daryoush Saeed-Vafa: None; Juan Hernandez-Prera: None; Pedro Cano: None; James Saller: None; Bryan McIver: *Speaker*, Eli Lilly; *Consultant*, Eisai Pharmaceuticals, Blueprint Medicines, Exelixis; *Advisory Board Member*, NCCN; Theresa Boyle: None

Background: Medullary thyroid carcinoma (MTC), a malignancy with frequent *RET* mutations, can occur either sporadically or within the spectrum of multiple endocrine neoplasia (MEN) syndrome. Splice site variants (SSVs) can result in production of truncated, albeit still functional proteins, through exon skipping. Since patients with metastatic *RET*-mutant MTC can benefit from targeted treatments, the scope of this study was to explore the frequency and potential significance of SSVs in MTC.

Design: The observation of detectable *RET* SSVs in routine cases of MTC led to an extended retrospective search of patients with a diagnosis of MTC and molecular testing results. DNA and RNA next generation sequencing (NGS) was performed on the Illumina TruSight Tumor 170 (Illumina Inc., San Diego, CA) platform, a 170-gene panel designed to identify actionable molecular alterations in solid tumors. Nucleic acids were extracted from macrodissected unstained formalin-fixed paraffin-embedded surgical specimen tissue sections, after annotation for tumor cellularity enrichment.

Results: We identified 14 patients, mostly middle-aged (median: 51 years; range 27-71) women (10/14; 71.4%), with advanced MTC. Despite having small tumors (mean size 2.87 ± 1.24 cm), all patients (14/14; 100%) were node-positive and four (4/14; 28.6%) had distant metastases at presentation. Eventually, almost all (13/14; 92.9%) developed metastases to the bones, liver, and lungs. One patient (1/14; 7.1%) had MEN2A syndrome due to a heterozygous *RET* p.C618S germline mutation. Most patients (12/14; 85.7%) had *RET*-altered tumors, with p.M918T as the most frequent mutation (6/12; 50%). Two patients without *RET* alterations (2/14; 14.3%) had *HRAS* mutations (p.G13R and p.Q61R). A total of 28 *RET* SSVs were detected in 11/13 (84.6%) of evaluable tumors including 8/10 (80%) of *RET*-mutant and 2/2 (100%) *HRAS*-mutant tumors, all of which had the t(10;10)(q11.2;q11.2)(chr10:g.43596172::chr10:g.43600398) SSV resulting in *RET* exon 3-7 skipping. The remaining cases (2/13; 15.4%) did not have detectable *RET* SSVs, but had very low tumor cellularity and *RET*-mutation variant allele frequency.

Conclusions: Irrespective of the driving mutation, SSVs in *RET* occurred in high frequency in MTC. The identification of *RET* SSVs in MTC might represent a novel diagnostic feature for this tumor and may represent an opportunity for better understanding its pathogenesis. Additional work is needed to explore any potential options for targeted therapy for MTC with *RET* SSVs.

358 Clinicopathological Characteristics of Low to Intermediate Grade Neuroendocrine Tumors with Oncocytic Features

Shengjie Cui[1], John Paulsen Jr.[1], Bella Liu[1], Kevin Mijares[2], Jing Han[2], Jihong Sun[3]
[1]Icahn School of Medicine at Mount Sinai, New York, NY, [2]Icahn School of Medicine at Mount Sinai St Luke's-Roosevelt Hospital Center, New York, NY, [3]Mount Sinai West, New York, NY

Disclosures: Shengjie Cui: None; John Paulsen Jr.: None; Bella Liu: None; Kevin Mijares: None; Jing Han: None; Jihong Sun: None

Background: Neuroendocrine tumors (NET) with oncocytic features are rare. To date, few studies have described the metastatic characteristics of these tumors, most of which were limited by the low number of cases. One article characterized intermediate to high grade (G2 and G3) oncocytic NET of the pancreas with an ominous outcome; however, metastatic features of low grade oncocytic NET has, to our knowledge, been hitherto unexplored. Our study characterized the clinical and metastatic features of 32 low to intermediate grade oncocytic NET of various organs.

Design: The pathology database was queried to identify 32 low to intermediate grade oncocytic NET from 2000-2021. Metastatic rate of our cases was compared with that of a retrospective study in which 7,334 patients with low to intermediate NET of various organs were included.

Results: Mean patient age is 60.7 years (range: 29-81; 1 patient without age information was excluded). The male to female ratio is 11:21. Primary site of the tumor includes small bowel/ileocecum (n=10), lung (n=6), thymus (n=3), stomach (n=2), pancreas (n=1), kidney (n=1), and unknown (n=9; including metastatic cases that origin of primary tumor was not identified and metastatic cases without clinical history provided). 15 cases were low grade (G1/typical) NET with oncocytic features and 8 cases were intermediate grade (G2/atypical) NET with oncocytic features. The remaining 9 cases were with unknown primary site, precluding classification into a particular grade category. The overall metastatic rate is 84.4%, which is much higher than that of the NET from the retrospective study (84.4% vs 23%, $p < 0.0001$). The most frequent metastatic site is liver (59.3%), followed by lymph node (33.3%). Interestingly, NET from the retrospective study reported a much higher rate of liver metastasis than our study (82% vs 59.3%, $p = 0.0025$).

Table 1: Clinicopathological characteristics of low to intermediate grade oncocytic NET.

Pt	Age	Sex	Primary site	Met site(s)	MIB-1 /Ki-67	Mitosis /necrosis	Grade /Classification
1	29	F	Small bowel (typical)	LN	<1%	No	G1
2	44	M	Small bowel (typical)	* extends to mesentery	5%	No	G2
3	77	F	Small bowel (typical)	mesenteric implants	<1%	No	G1
4	79	F	Ileum (typical)	LN, mesentery, peritoneum	<1%	No	G1
5	72	F	Ileum (typical)	LN, omentum	1%	No	G1
6	71	F	Terminal ileum	Liver, omentum, mesentery, b/l tube&ovary (typical)	5%	2MF/10HPF	G2
7	78	F	Ileocecum (typical)	Liver, mesentery	2%	No	G1
8	54	F	Ileum, cecum, appendix (typical)	LN	<1%	No	G1

9	57	F	Ileocecum, R colon	Liver (typical), LN, omentum, mesentery, peritoneum	8%	No	G2
10	53	M	Ileocecal valve (typical)	LN	4%	No	G2
11	59	F	Lung (typical)	LN	Up to 5%	Low MF	Typical
12	68	M	Lung	Liver (typical)	<2%	<2MF/10HPF	Typical
13	58	M	Lung (typical)	Liver (typical)	<1%	No	Typical
14	53	F	Lung	NA	NA	NA	Typical
15	64	M	Lung	Liver (typical)	5%	No	Typical
16	57	M	Lung	Liver (typical)	5%	No	Typical
17	70	M	Thymus (typical)	Bone, stomach	5-10%	No	Typical
18	83	F	Thymus (atypical)	NA	5%	2MF/10 HPF	Atypical
19	40	M	Thymus (atypical)	LN, *extends to lung & pericardium	5%	2MF/ 10HPF	Atypical
20	55	M	Stomach (typical)	NA	NA	No	G1
21	70	F	Stomach	NA	<3%	<2/mm2	G1
22	55	F	Pancreas	Liver (atypical)	~20%	7MF/10 HPF	G2
23	56	F	Kidney (atypical)	b/l ovary/pelvis	NA	3MF/10HPF, foci of necrosis	G2
24	81	F	NA	LN (typical)	6%	1-2MF /10HPF	Typical
25	51	F	NA	Liver (typical)	<1%	1MF/10hpf	Typical
26	51	F	NA	Liver, b/l ovary, peritoneum	NA	focal necrosis	Atypical
27	47	M	NA	Liver (atypical)	30%	2MF/10 HPF	Atypical
28	52	F	NA	Liver (atypical)	10%	2MF/10 HPF	Atypical
29	66	F	NA	Liver (atypical)	20%	2MF/10 HPF	Atypical
30	66	F	NA	Liver (G1/G2), pancreas, bone	8%	1MF/10HPF	G1/G2
31	66	M	NA	Liver (atypical)	10%	foci of necrosis	Atypical
32	NA	F	NA	Liver (atypical)	NA	>2MF/10HPF	Atypical

Abbreviations: Pt: patient; F: female; M: male; LN: lymph node; MF: mitotic figures; HPF: high power field. * Not counted for metastasis.

Conclusions: Our study summarized the clinical and the metastatic characteristics of low to intermediate grade oncocytic NET that were diagnosed at our institution over the past 20 years. Identifying a NET as having oncocytic features may better assist patient management.

359 NUTM1-Rearranged Carcinomas of the Thyroid: A Distinct, Less Aggressive Subset of NUT Carcinoma

Steven Gilday[1], Michelle Afkhami[2], Nicole Chau[3], Nicole Cipriani[4], Ronald Ghossein[5], Alan Kramer[6], Sewanti Limaye[7], Carlos Lopez[8], Bin Xu[5], Songlin Zhang[9], Christopher French[1], Justine Barletta[1]
[1]Brigham and Women's Hospital, Harvard Medical School, Boston, MA, [2]City of Hope National Medical Center, Duarte, CA, [3]BC Cancer, Vancouver, Canada, [4]University of Chicago, Chicago, IL, [5]Memorial Sloan Kettering Cancer Center, New York, NY, [6]San Francisco, CA, [7]Kokilaben Ambani hospital, Mumbai, India, [8]Northwell Health, Lake Success, NY, [9]The University of Texas Health Science Center at Houston, Houston, TX

Disclosures: Steven Gilday: None; Michelle Afkhami: None; Nicole Chau: None; Nicole Cipriani: None; Ronald Ghossein: None; Alan Kramer: None; Sewanti Limaye: None; Carlos Lopez: None; Bin Xu: None; Songlin Zhang: None; Christopher French: None; Justine Barletta: None

Background: NUT carcinoma is a rare subtype of squamous cell carcinoma defined by *NUTM1* fusions (the most frequent fusion partners are *BRD4*, *BRD3*, and *NSD3*, present in roughly 80%, 15% and 5% of cases, respectively) that characteristically presents in midline structures of the head and neck or thorax of young patients and carries a very poor prognosis, with a median survival of 6.5 months and a 2-year overall survival rate of 19-22%. Only rare cases of NUT carcinoma involving the thyroid have been reported.

Design: We identified 9 cases of NUT carcinoma diagnosed between 1999 and 2021 that arose within the thyroid (2 cases previously published) and evaluated clinical characteristics, histopathologic features, immunohistochemical profile, *NUTM1* fusion partner, and outcome.

Results: The median patient age at diagnosis was 35 years (range 17-72 years). There were 6 female and 3 male patients. The mean tumor size was 4.4 cm (range 2.5-6.0 cm). A diagnosis of NUT carcinoma was made at the time of biopsy or resection in 4 (44%) cases, whereas 3 cases were diagnosed as poorly differentiated thyroid carcinoma (PDTC) and 2 as anaplastic thyroid carcinoma (ATC). Squamous differentiation was present in 57% of cases (4/7; 2 cases had no slides available for review). For cases with immunohistochemistry results, all (4/4) were positive for NUT on biopsy or resection, 57% (4/7) for TTF1, 40% (2/5) for PAX8, and 75% (3/4) for p63 or p40. All 4 cases with PD-L1 staining showed a combined positive score of 1% or higher (range 5-100). The *NUTM1* fusion partner was *NSD3* in 6 (67%) cases, *BRD4* in 2 (22%) cases, and unknown in 1 (11%) case. Total or hemithyroidectomy was performed in 7 cases (all of which showed gross extrathyroidal extension), and 2 cases underwent biopsy only. Lymph node and distant metastases were present at diagnosis in 7 patients and 1 patient (uncertain in 3 patients), respectively. At last follow up, only 2 patients had died of disease (3.5 months and 31 months after diagnosis), 3 were alive with disease, and 3 were alive with no evidence of disease (36.2 month median follow-up time for patients alive at last follow up). For our cohort, the median overall survival was not reached. For patients with sufficient follow up, the 2-year survival rate was 83%.

Conclusions: NUT carcinoma of the thyroid has potential histologic and immunohistochemical overlap with PDTC and ATC and appears to have a significantly higher rate of *NSD3-NUTM1* fusions and a longer survival than typical NUT carcinomas.

360 A Subset of Anaplastic Thyroid Carcinomas with Abnormal p16 Immunohistochemistry Demonstrate MTAP Loss

Robert Humble[1], Nathanael Christensen[1], Andrew Bellizzi[1]
[1]*University of Iowa Hospitals & Clinics, Iowa City, IA*

Disclosures: Robert Humble: None; Nathanael Christensen: None; Andrew Bellizzi: None

Background: Anaplastic thyroid carcinoma (ATC) is a rare, aggressive variant of thyroid cancer, often arising from a pre-existing well-differentiated thyroid carcinoma (WDTC) component. The mechanism of WDTC to ATC transformation is poorly understood. A previous study identified abnormal p16 expression in a significant portion of anaplastic thyroid carcinomas, suggesting a role for CDKN2A/p16 in the evolution to ATC (PMID: 32683537). Loss of p16 immunohistochemistry (IHC) is not specific for CDKN2A homozygous deletion. Methylthioadenosine phosphorylase (MTAP) is located adjacent to CDKN2A on chromosome 9p21 and is frequently co-deleted. In malignant mesothelioma, MTAP loss is used as a reliable surrogate for CDKN2A homozygous deletion. To our knowledge, MTAP has not been examined in ATC.

Design: p16 (clone EGH4) and MTAP (clone 2G4) IHC was performed on tissue microarrays (TMAs) and whole sections (WS) constructed from ATC resections and biopsies (n=28); when present the co-occurring WDTC component was also represented (n=15). TMAs were also constructed from separate papillary thyroid carcinomas (PTC, n=22) and follicular thyroid carcinomas (FTC, n=22) without an ATC component. p16 IHC was assessed as wild-type, null (complete absence of staining), or overexpressed (>/=70%). MTAP was assessed as intact or lost. Survival analysis was performed using Kaplan-Meier curves and the log-rank test.

Results: p16 IHC results were available for 26/28 ATC cases, with 81% (n=21) showing null staining; corresponding matched WDTCs were wild-type (n=6) or null (n=3). MTAP IHC results were available for 27/28 ATC cases, with 22% (n=6) showing loss of staining; available corresponding matched WDTCs showed MTAP loss in 33% of cases (n=2). MTAP loss was not associated with survival. p16 IHC was wild-type in 95% of PTCs (n=18) and 50% of FTCs (n=7) and null in 5% of PTCs (n=1) and 43% of FTCs (n=6). MTAP was intact in all PTCs (n=20) and FTCs (n=19). Detailed data are presented in the Tables below.

Table 1 p16 and MTAP IHC for ATC, matched WDTC, and unmatched PTC, FTC

		ATC	Matched WDTC	PTC	FTC
p16	Null	21	5	1	6
	Wild-type	1	6	18	7
	Overexpressed	4	1	0	1
MTAP	Intact	21	12	20	19
	Lost	6	2	0	0

Table 2 p16 and MTAP IHC in ATC

	MTAP intact (n)	MTAP lost (n)
p16 null (n)	15	5
p16 wild-type/ overexpressed (n)	4	1

Conclusions: In our study MTAP loss was restricted to ATC, which occurred in 25% of tumors with null pattern p16 staining. Although apparent null pattern p16 was frequent in FTC (and rare in PTC), MTAP was uniformly intact. Our findings suggest that MTAP IHC may be more specific for a genetic CDKN2A abnormality than p16 IHC, as has been demonstrated previously in mesothelioma. MTAP status did not predict survival.

361 Solitary Fibrous Tumor (SFT) of the Adrenal Gland: A Multi-institutional Study of Nine Cases with Literature Review

Shilpy Jha[1], Subhasini Naik[2], Manas Baisakh[3], Anandi Lobo[4], Shivani Sharma[5], Ekta Jain[5], Bonnie Balzer[6], Indranil Chakrabarti[7], Anil Parwani[8], Biswajit Sahoo[9], Sourav Mishra[1], Nakul Sampat[1], Niharika Pattnaik[1], Romila Tiwari[1], Sambit Mohanty[1]

[1]Advanced Medical and Research Institute, Bhubaneswar, India, [2]Prolife Diagnostics and Apollo Hospitals, Bhubaneswar, India, [3]Apollo Hospitals, Bhubaneswar, India, [4]Kapoor Centre of Urology and Pathology, Raipur, India, [5]Core Diagnostics, Gurgaon, India, [6]Cedars-Sinai Medical Center, Los Angeles, CA, [7]North Bengal Medical College, India, [8]The Ohio State University, Columbus, OH, [9]All India Institute of Medical Sciences, Bhubaneswar, India

Disclosures: Shilpy Jha: None; Subhasini Naik: None; Manas Baisakh: None; Anandi Lobo: None; Shivani Sharma: None; Ekta Jain: None; Bonnie Balzer: *Consultant*, Core Diagnostics, Castle Biosciences, PathologyWatch; Indranil Chakrabarti: None; Anil Parwani: None; Biswajit Sahoo: None; Sourav Mishra: None; Nakul Sampat: None; Niharika Pattnaik: None; Romila Tiwari: None; Sambit Mohanty: None

Background: SFT is a mesenchymal neoplasm of the soft tissue and viscera with inv12(q13q13)-derived *NAB2–STAT6* fusion resulting in the nuclear expression of STAT6. Primary SFT of the adrenal gland is rare and only 12 cases have been reported in the literature as isolated case reports and rare small series, and the diagnoses were primarily based on CD34 immunohistochemistry (IHC). STAT6 IHC and *NAB2–STAT6* rearrangement was studied in only in two tumors. Also, risk stratification model to assess the propensity to develop metastasis was not described on any of the previously described tumors.

Design: We add a series of 9 patients to the collection of adrenal SFT where the clinicopathologic parameters including clinical presentation, imaging, histopathology, IHC, and molecular profiles, and management and follow-up data were analyzed comprehensively.

Results: The results are illustrated in figures 1 and 2 as follows. Figure 1 shows the demographics, histopathologic, IHC, molecular, treatment, risk stratification, and follow-up data on the cases of adrenal SFT, including the present cohort of 9 cases (abbreviations used: NA: Not available; ND: Not done; LTF: Lost to follow-up; IHC: Immunohistochemistry). Figure 2 shows a case of adrenal SFT (a: Hematoxylin and Eosin stain; b: STAT6 expression; c: CD34 expression; d: STAT6 FISH break apart assay.

Figure 1 - 361

Patients	Age/ Gender	Laterality	Maximum dimension of the tumor (cm)	Cell Type	CD34 IHC	STAT6 IHC	Molecular Profile	Treatment	Follow-up	Vital status	Risk class
Case 1	46/M	Left	7	Spindle	Positive	Positive	ND	Resection	7 months	Alive	Low
Case 2	44/M	Right	5	Spindle	Positive	Positive	NAB2-STAT6	Resection	10 months	Alive	Low
Case 3	70/M	Left	2.5	Spindle	Negative	Positive	ND	Resection	23 months	Alive	Low
Case 4	61/F	Left	3	Spindle	Positive	Positive	NAB2-STAT6	Resection	13 months	Alive	Low
Case 5	55/M	Right	2	Spindle	Positive	Positive	ND	Resection	LTF	LTF	Low
Case 6	64/M	Left	5	Spindle	Negative	Positive	ND	Resection	29 months	Alive	Low
Case 7	27/F	Right	7	Spindle	Positive	Positive	ND	Resection	LTF	LTF	Low
Case 8	58/F	Right	10.5	Spindle	Positive	Positive	ND	Resection	7 months	Alive	Intermediate
Case 9	19/M	Left	4	Spindle	Positive	Positive	NAB2-STAT6	Resection	9 months	Alive	Low
Prévot et al	42/F	Right	NA	Round	Positive	ND	ND	Resection	NA	NA	Cannot be determined
Bongiovanni et al.	23/F	Left	9	Spindle	Positive	ND	ND	Resection	NA	NA	Low
Shen et al.	51/M	Left	6	Spindle	ND	ND	ND	Resection	NA	NA	Cannot be determined
Kakihara 15	39/F	Left	10	Spindle	Positive	ND	ND	Resection	20 months	Alive	Low
Ho et al.	71/M	Right	15.5 (gross)	Spindle	Positive	ND	ND	Resection	NA	NA	High
Toniato et al.	54/M	Bilateral	15	Spindle	Positive	ND	ND	Resection	18 months	Alive	Low
Conzo et al.	52/F	Right	9	Spindle	Positive	ND	ND	Resection	8 months	Alive	Low
Treglia et al.	33/M	Right	3	Spindle	Positive	ND	NA	Resection	NA	NA	Low
Kouba et al.	58/M	NA	9	NA	Positive	Positive	NAB2-STAT6	Resection	60 months	NA	Intermediate
Yao et al.	68/M	Right	6	Cuboidal	Positive	Positive	NAB2-STAT6	Resection	6 months	Alive	Intermediate
Gebresellassie et al.	13/F	Right	19	Spindle	ND	ND	ND	Resection	3 months	Alive	Intermediate
Yoni et al.	52/M	Right	11	Spindle	Positive	ND	ND	Resection	36 months	Alive	Low

Figure 2 – 361

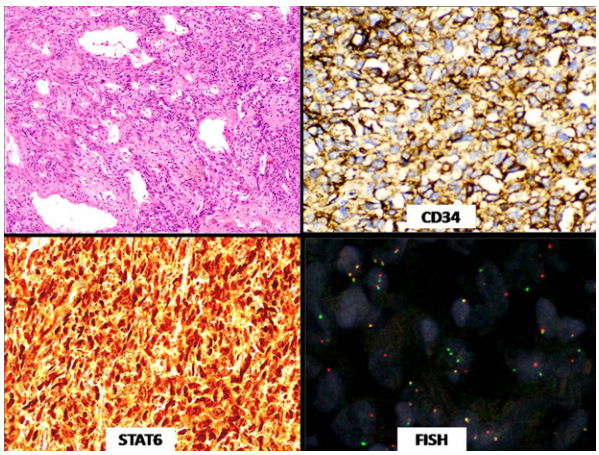

Conclusions: 1. Based on our experience with the largest series of adrenal SFT to date and aggregate of the published data, SFTs of the adrenal are predominantly spindle cell neoplasms with indolent behavior with wide age distribution (13 to 71 years) and a slight male preponderance.

2. Majority of the tumors fall into the low-risk (75%, 12/16) and only 4 (25%, 4/16) belonged to intermediate-risk categories. None belonged to the high-risk class.

3. Owing to its rarity and wide age distribution, the differential diagnosis is broad and requires a thorough IHC work up that should include STAT6.

362 Prediction Model for Lymph Node Metastasis Based on DNA Methylation Markers Using Deep Learning-Based Model in Follicular Cell-Derived Neoplasm

Chan Kwon Jung[1], Jong-Lyul Park[2], Sora Jeon[3], Ja-Seong Bae[4], Yong Sung Kim[5]
[1]The Catholic University of Korea, Seoul St. Mary's Hospital, Seoul, South Korea, [2]The Korea Research Institute of Bioscience and Biotechnology, Daejeon, South Korea, [3]Cancer Research Institute, College of Medicine, The Catholic University of Korea, Seoul, South Korea, [4]College of Medicine, The Catholic University of Korea, Seoul, South Korea, [5]Daejeon, South Korea

Disclosures: Chan Kwon Jung: None; Jong-Lyul Park: None; Sora Jeon: None; Ja-Seong Bae: None; Yong Sung Kim: None

Background: Lymph node metastasis is the main risk factor for the recurrence of thyroid cancer. We aimed to develop a deep learning-based prediction model for the prediction of lymph node metastasis of thyroid cancer using DNA methylation markers, regardless of sample type and method of sample collection.

Design: A total of 507 patients with thyroid nodules were enrolled in this study. Follicular cell-derived thyroid neoplasms included benign (n=166), noninvasive follicular thyroid neoplasms with papillary-like nuclear features (n=77), and malignant tumors (n=264). DNA was extracted from fresh, fresh frozen, or formalin-fixed paraffin-embedded tissue samples. DNA methylation levels for three markers (cg10705422, cg17707274, and cg26849382) were analyzed by the bisulfite modification-based pyrosequencing assay. A neural network model was trained with a training data set of 354 patients and tested with a test set of 153 patients. Input variables were three DNA methylation markers, specimen type, sex, age, and cell type (conventional vs. oncocytic cells).

Results: DNA methylation levels of three markers were significantly lower in thyroid cancers than in non-malignant tumors. In the test set, the performance of the neural network algorithm achieved an area under the receiver operating characteristic (AUROC) of 0.928, with a sensitivity of 97.4%, specificity of 87.7%, a negative predictive value of 99.0%, and a positive predictive value of 73.1%.

Conclusions: The deep learning model based on DNA methylation levels could accurately predict lymph node metastasis in patients with thyroid cancer. This prediction model may help surgeons to decide whether to perform cervical lymph node dissection.

363 Cost-Analysis of ThyroSeq Molecular Testing: A Real-World Institutional Experience

Hannah Lee[1], Elham Khanafshar[1], Britt-Marie Ljung[1], Mohsen Hosseini[1]
[1]University of California, San Francisco, San Francisco, CA

Disclosures: Hannah Lee: None; Elham Khanafshar: None; Britt-Marie Ljung: None; Mohsen Hosseini: None

Background: Fine needle aspiration biopsy is the primary pre-surgical tissue diagnosis modality for thyroid nodules, yet indeterminate in up to 25% of cases. ThyroSeq Genome Classifier test provides a means to risk-stratify thyroid nodules and guide management. We assessed the performance and cost-effectiveness of ThyroSeq testing for cytologically indeterminate nodules in our health system.

Design: We identified cytologically indeterminate thyroid nodules (Bethesda categories III-V) at our institution that had undergone ThyroSeq test from 2019 to 2021. The results of ThyroSeq and consequent clinical management, including surgical pathology reports of thyroid resections, were reviewed (Table 1).

Results: We identified 341 nodules that underwent ThyroSeq testing (Table 1). Positive ThyroSeq results were reported in 110 nodules with rates of 27% in atypical, 41% in follicular lesion, and 83% in suspicious nodules (Bethesda categories III, IV, and V). 84 of ThyroSeq positive patients (76%) had a surgical resection, while only 36 patients with negative ThyroSeq results (16%) underwent surgery. Based on surgical pathology examination of the resection specimen, the sensitivity and specificity of ThyroSeq for detecting high-risk lesions were 92% and 53%, respectively, with an accuracy of 0.71. Overall, ThyroSeq utilization led to a 65% reduction (120 vs. 341) in diagnostic thyroidectomy by incurring a cost of approximately $5,200 per surgery avoided (compared to an estimated average national cost of $19,500 for a thyroidectomy).

Table 1. Summary of ThyroSeq testing for indeterminate thyroid nodules at UCSF (2019-2021)

Bethesda Category	Cases	TP (%)	TS Risk % (Mean)	Most Common Molecular Findings	TPS (% of TP)	TNS (% of TN)	TS Sensitivity	TS Specificity
III	229	62 (27%)	33-99 (62%)	NRAS p.Q61K/R; HRAS p.Q61K/R; DICER1 p.E1813G; TERT p.C250T; THADA/IGF2BP3 fusion	45 (73%)	27 (16%)	90%	64%
IV	106	43 (41%)	30-99 (64%)	NRAS p.Q61K/R; HRAS p.Q61K/R; HRAS p.G13R; DICER1 p.E1705I/K; TERT p.C228T	35 (81%)	9 (14%)	95%	35%
V	6	5 (83%)	91-99 (96%)	BRAF p.V600E	4 (80%)	0 (0%)	-	-
Sum	341	110			84	36	92%	53%

TS, ThyroSeq; TP, ThyroSeq positive cases; TN, ThyroSeq negative cases; TPS, ThyroSeq positive cases with consequent surgery; TNS, ThyroSeq negative cases with subsequent surgery

Conclusions: ThyroSeq showed similar sensitivity but lower specificity compared to prior studies. This could be due to an increased mutation detection rate in adenomatoid nodules and adenomas or a random sampling variation. ThyroSeq utilization drastically reduced the need for surgery and was justifiable from a pure cost-analysis standpoint.

364 The Role of Genomic and Epigenomic factors in Thyroid Follicular Cell Neoplastic Progression

Cody Marshall[1], Tanvi Verma[1], Kossivi Dantey[2], Joseph DelTondo[2], Sydney Finkelstein[3]
[1]Allegheny Health Network, Pittsburgh, PA, [2]Allegheny General Hospital, Pittsburgh, PA, [3]Interpace Diagnostics, Pittsburgh, PA

Disclosures: Cody Marshall: None; Tanvi Verma: None; Kossivi Dantey: None; Joseph DelTondo: None; Sydney Finkelstein: None

Background: Most genomic mutations detected in cytology indeterminate thyroid nodules can be present in both benign or malignant lesions. Moreover, a small subset (10-15%) of malignant nodules will lack detectable genomic mutational change. Thus neoplastic progression involves epigenomic growth regulation that determine ultimate phenotypic status as benign vs. malignant.

Design: Using a broad panel of growth promoting (6) and suppressing (5) microRNA (miRNA) markers to evaluate epigenomic pathobiology, we compared the cumulative pattern and individual growth promoting/suppressing miRNA pairwise relationships to better understand the role of epigenomics in non-mutated and mutated thyroid nodules with indeterminate cytology (Bethesda Diagnostic Category III and IV).

The preoperative needle aspirates of 58 cytology indeterminate nodules with known surgical pathology outcome underwent quantitative PCR for 11 specific miRNAs with established growth promoting and growth suppressing properties. Mutational analysis used next generation sequencing for a broad marker panel (10 oncogenes, 38 translocations). Overall and individual marker quantitation was performed as well as pairwise determination of relative expression of growth promoting/suppressing pairs. A cohort of 50 benign follicular cell nodules (nodular hyperplasia, follicular adenoma) provided the quantitative basis for defining benign disease status

Results: Of 26 nodules without detectable mutational change, 22 were benign and 4 malignant. Of 32 nodules with RAS-like mutations, 16 were benign and 16 were malignant. The averaged expression level of growth promoting and suppressing miRNAs was higher in malignant versus benign for both mutated and non-mutated nodules. Similarly overall growth promoting/suppressing pair status was higher in malignant vs. benign nodules. Of note, the quantitative difference between benign vs. malignant nodules was less in RAS-like mutated vs. non-mutated nodules as was the quantitative expression of individual miRNAs.

Conclusions: Epigenomic factors such as miRNA expression contributes to ultimate phenotypic expression of thyroid nodules in both mutated as well as non-mutated lesions. The biological effect of differential miRNA expression appears greater in non-mutated thyroid nodules where it can play a relatively greater role in determining benign versus malignant status. Multistep carcinogenesis include epigenetic changes which may serve as critical determinant of malignant transformation.

365 Cauda Equina Neuroendocrine Neoplasms are Unique Lumbar Spine Neoplasms of Uncertain Cytogenesis

Ozgur Mete[1], Biswarathan Ramani[2], Arie Perry[2], Sylvia Asa[3]
[1]University Health Network, University of Toronto, Toronto, Canada, [2]University of California, San Francisco, San Francisco, CA, [3]Case Western Reserve University/University Hospitals Cleveland Medical Center, Cleveland, OH

Disclosures: Ozgur Mete: None; Biswarathan Ramani: None; Arie Perry: None; Sylvia Asa: *Advisory Board Member*, Leica Biosystems; *Consultant*, Iron Mountain; *Advisory Board Member*, Ibex Medical Analytics; *Consultant*, PathAI

Background: The tumor known as “cauda equina paraganglioma” is a neuroendocrine neoplasm that arises in the lumbar spine. Recent data suggest that unlike other paragangliomas, it expresses keratins and does not have loss of SDHB. We further investigated a large series of these tumors.

Design: Tumors classified as “cauda equina paraganglioma” were retrieved from two institutions. Retrospective data including a number of biomarkers of neural and neuroendocrine neoplasms were collected; in some cases, additional immunostains were applied to archived materials.

Results: We collected 24 tumors that had been classified as cauda equina paraganglioma including select data from 17 previously published cases (1). There were 8 female and 16 male adult patients, with a median age of 47 years. The majority were composed

of solid sheets and nests of epithelioid cells; 6 had scattered ganglion cells. Neurofilament staining was identified in ganglion cells. GFAP was negative with a few exceptions with focal positivity, likely representing trapped nontumorous tissue. All tumors tested were positive for synaptophysin, chromogranin-A and CD56 as well as at least one keratin (AE1/AE3, CAM5.2); staining for EMA (with the exception of one with perinuclear reactivity), CK7 and CK20 were negative in a few cases tested. All tumors were consistently negative for GATA3. Of 5 tumors tested with tyrosine hydroxylase, 3 had focal reactivity and one had variable reactivity. S100 protein was identified with variable positivity, mainly highlighting sustentacular cells. All tumors tested were negative for transcription factors found in various other epithelial neuroendocrine neoplasms including TTF1, CDX2, PIT1, TPIT, SF1, and monoclonal PAX8. A subset of tumors expressed focal PSAP. Among tested tumors, positive staining was also found in a few tumors for serotonin, and one with pancreatic polypeptide, while glucagon, peptide YY and monoclonal CEA were negative. SDHB was consistently intact. The median Ki67 LI was 4.5% (range: 1-15%).

Conclusions: Despite the limited data showing focal/variable tyrosine hydroxylase expression, the “cauda equina paraganglioma” does not qualify as a paraganglioma based on current definitions, but rather represents a distinct neuroendocrine neoplasm of uncertain cytogenesis, that can, on occasion, be a composite tumor with neuronal elements.

(1). Ramani et al. Acta Neuropathol. 2020 Dec;140(6):907-917.

366 The Enigmatic Association of Brown Adipose Tissue with Pheochromocytoma

Aysha Mubeen[1], Sofia Canete-Portillo[2], Samuel Galgano[2], Soroush Rais-Bahrami[2], Cristina Magi-Galluzzi[2]
[1]Brigham and Women's Hospital, Boston, MA, [2]The University of Alabama at Birmingham, Birmingham, AL

Disclosures: Aysha Mubeen: None; Sofia Canete-Portillo: None; Samuel Galgano: None; Soroush Rais-Bahrami: None; Cristina Magi-Galluzzi: None

Background: Brown adipose tissue (BAT) is present in infancy and regresses with age. Catecholamine excess induced by pheochromocytomas (PCC) has been postulated to cause BAT activation. BAT activation in PCC has been reported in radiology literature; however, pathology focused studies have been sparse. We aimed to analyze the presence of BAT in a cohort of PCC and to evaluate their clinicopathologic features.

Design: Slides from 65 consecutive PCC diagnosed between 2015 and 2020 were reviewed for the presence of BAT. BAT was classified as ‘focal’ if present on one slide, or ‘prominent’ if present on more than one slide. A detailed review of clinicopathologic features was also performed.

Results: BAT was identified in 19/65(29%) patients (11 females and 8 males) and was prominent in 8 (42%) cases with a hibernoma-like appearance. Patients’ median age was 50.7 years (range: 28-70); 4 patients were African Americans and 15 Whites. Mean body mass index was 26.60kg/m^2 (range:17.79- 40.88). Tumors’ mean size was 4.6 cm (range: 1.9-9.5). On imaging, one tumor showed significant fat stranding. Three cases were notable for intraoperative findings suggesting "retrocaval extension or desmoplastic reaction around tumor". Mean follow up was 20.8 months (range: 1-66).

Prominent BAT was grossly identified as peri-adrenal brown, fleshy tissue akin to hibernoma; microscopically cells displayed granular, multivacuolated cytoplasm (Figure 1). SDHB immunohistochemistry was available in 17(89%) cases and showed retained expression. Genetic testing results were available for 7 (37%) patients: 4 showed NF1 (neurofibromatosis 1) mutation, 1 showed RET (rearranged during transfection) mutation (MEN2A), and 2 showed no mutations. At follow-up, 2 (11%) patients had metastatic disease (lymph node, spine and liver); 17 showed no evidence of disease. One of 2 patients with metastatic disease had NF1 with an additional ERCC2 (excision repair cross-complementing in rodents 2) mutation on molecular analysis.

Figure 1 - 366

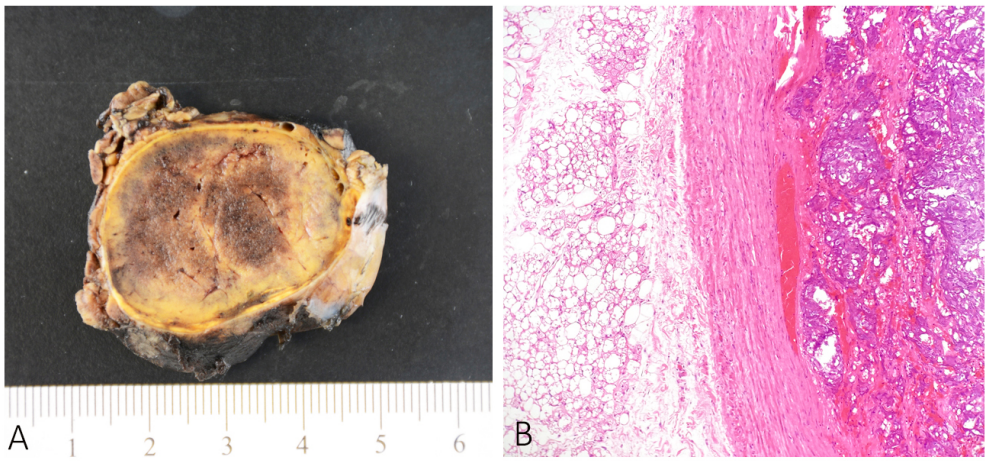

Conclusions: BAT was present in more than a quarter of PCC examined and was prominent in a subset. Awareness of the association of BAT with PCC, especially when prominent, is important, as tumors may have a more ominous appearance radiologically and intraoperatively. BAT activation (detected by Positron Emission Topography) has been reported to be associated with poor survival in PCC. Further investigation is needed to see if BAT activation corresponds to characteristic histologic features.

367 Paragangliomas of Cauda Equina Show Only Limited Epithelial Phenotype and Distinct Immunohistochemical Features from Other Paragangliomas and Neuroendocrine Tumors

Jiri Soukup[1], Monika Manethova[1], Jan Drugda[1], Ales Kohout[1], Hana Faistova[1], Hana Vosmikova[1], Petra Kasparova[1], Radka Dvorakova[1], Boris Rychly[2], Markéta Trnková[3], Ludmila Michnova[4], Barbora Vitovcova[5], Miroslav Kaiser[6], Jan Kozak[7], Petr Vachata[8], David Netuka[9], Martin Kanta[1], Filip Gabalec[1], Tomas Cesak[1]

[1]University Hospital and Faculty of Medicine Hradec Kralove, Charles University, Hradec Kralove, Czech Republic, [2]Alpha Medical, s. r. o., [3]AeskuLab Patologie k.s., Czech Republic, [4]Military University Hospital Prague, Czech Republic, [5]Faculty of Medicine Hradec Kralove, Charles University, Hradec Kralove, Czech Republic, [6]The Regional Hospital Pardubice, Pardubice, Czech Republic, [7]National Oncology Institute of Slovakia, Bratislava, Slovakia, [8]Masarykova Nemocnice Usti nad Labem, Usti nad Labem, Czech Republic, [9]Military University Hospital Prague and 1st Medical Faculty, Charles University, Prague, Czech Republic

Disclosures: Jiri Soukup: None; Monika Manethova: None; Jan Drugda: None; Ales Kohout: None; Hana Faistova: None; Hana Vosmikova: None; Petra Kasparova: None; Radka Dvorakova: None; Boris Rychly: None; Markéta Trnková: None; Ludmila Michnova: None; Barbora Vitovcova: None; Miroslav Kaiser: None; Jan Kozak: None; Petr Vachata: None; David Netuka: None; Martin Kanta: None; Filip Gabalec: None; Tomas Cesak: None

Background: Paragangliomas of cauda equina (PGCE) are distinct tumors of spinal cord with unknown histogenesis and indolent behavior. They differ from the pheochromocytomas/paragangliomas (PCPG) with respect to their immunoprofile, genetic and methylation profile. In this study, we analyzed clinicopathological features of 18 PGCE and compared their immunohistochemical profile with other neuroendocrine tumors.

Design: Archival samples of PGCE, PCPG and neuroendocrine tumors (NET) were reviewed and selected for the construction of tissue microarrays (TMA). Whole sections of PGCE were evaluated. Clinical and radiological data of PGCE were retrieved from the archive. Immunohistochemical staining was performed on TMA, with a wide array of antibodies against epithelial, neuroendocrine, neuronal and other potentially important proteins. Expression was scored as positive or negative by two observers independently. $\chi 2$ or Fisher's exact (FE) tests were used with p-values <0.0025 considered significant (Bonferroni correction).

Results: In total, the cohort consisted of 38 PCPs, 55 NET and 18 PGCE in 4 women and 14 men. The average age at the time of surgery was 46.2 years, median age 41 years and it ranged between 21 and 80 years. All the tumors were localized in area between L2 and L5 vertebra. Mean largest diameter was 39 mm. In 3 tumors, invasion of local structures was observed, and one of these cases recurred 19 months after surgery. No metastatic disease was seen. On MRI, flow-void phenomenon could be identified in 5/14 cases. Tumors had uniform morphology and were composed of cells with atypias in alveolar, trabecular, or solid

pattern. Variable hyalinization, edema, hemosiderin deposits and calcifications were seen. In 4/18 cases, gangliocytic differentiation was observed. Mitotic activity was identifiable in 8/18 cases, it ranged from 1 to 11 per 10 HPF (median 2, average 3.5). No atypical mitoses were seen. In PGCE and PCPG, we observed no expression of claudin-4, ACTH, and calcitonin; all were positive for synaptophysin, chromogranin and INSM1. SDHB was lost in 3/38 of PCPG but in none of PGCE. Comprehensive IHC results are listed in table 1.

Results of Immunohistochemistry				
	PGCE	**PCPG**	**NET**	**p value**
CK AE1/3	18/18	0/38	55/55	**<0.001** χ^2
CK 8/18	18/18	0/38	50/50	**<0.001** χ^2
BER-EP4	0/18	0/38	52/53	**<0.001** χ^2
MOC31	2/18	0/38	49/49	**<0.001** χ^2
E-cadherin	0/18	0/37	53/53	**<0.001** χ^2
EMA	0/18	0/37	11/43	**<0.001** χ^2
CD138	2/18	6/38	24/51	**0.001** χ^2
CD15	0/18	27/38	ND	**<0.001** FE
GATA3	0/18	35/37	ND	**<0.001** FE
Neurofilaments (NFL)	3/18	3/35	ND	0.37 FE
Internexin-α	18/18	38/38	46/52	0.03 χ^2
NeuN	0/18	8/38	ND	0.04 FE
SSTR2A	18/18	34/38	ND	0.29 FE
SSTR3	17/18	38/38	ND	0.32 FE
SSTR5	18/18	0/38	ND	**<0.001** FE
CD99	14/18	0/35	ND	**<0.001** FE
SOX2	15/18	0/37	ND	**<0.001** FE
Nestin	0/18	4/38	ND	0.29 FE

Figure 1 - 367

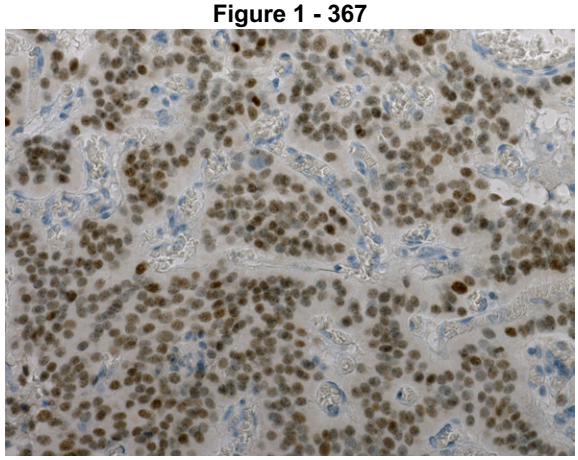

Conclusions: In contrast to PCPG, PGCE express cytokeratins, SOX2 (Figure 1), SSTR5 and CD99, while they lack expression of GATA3, CD15 and loss of SDHB. Except for cytokeratins, no expression of additional epithelial antigens (EpCAM, E-cadherin, CD138, EMA, claudin-4) was seen in PGCE, compared to NET. These findings underline a distinct nature of the entity with respect to NET and PCPG.

368 Differentiated High Grade Thyroid Follicular-cell Derived Carcinomas versus Poorly Differentiated Thyroid Carcinoma: A Clinicopathologic Analysis of 41 cases

Lester Thompson, Head and Neck Pathology Consultations, Woodland Hills, CA

Disclosures: Lester Thompson: None

Background: Criteria overlap for separating between malignant thyroid follicular epithelial cell derived neoplasms with high grade features of increased mitoses and tumor necrosis but lacking anaplastic histology. A reproducible Ki-67-based proliferation index has not been established.

Design: All cases (n=41) diagnosed as poorly differentiated (PDTC) or differentiated high grade thyroid follicular-cell derived carcinoma (DHGTC) were reviewed, with histologic features documented and mitotic figure counts and Ki-67 proliferation index performed. Outcome evaluation was performed to identify any differences.

Results: There were 17 DHGTC (9 papillary thyroid carcinoma [PTC]; 8 oncocytic follicular thyroid carcinoma [OTC]), with a median age of 64 years, with 9 females and 8 males. Tumors were large (median, 6.0 cm), usually unifocal (n=14), with only 1 tumor lacking invasion. Tumor necrosis was present in all; median mitotic count was 6/2 mm^2, with a median Ki-67 proliferation index of 8.2%. Three patients had metastatic disease at presentation, with additional metastases in 5 patients; 11 were alive (n=10) or dead (n=1) without evidence of disease (median, 21.2 months); with the remaining 6 patients alive (n=4) or dead (n=2) with metastatic disease (median, 25.8 months); overall median follow-up 23.9 months.

There were 24 PDTC, with a median age of 57.5 years, with 13 females and 11 males. Tumors were large (median, 6.9 cm), with 50% part of multifocal disease, with 3 tumors lacking invasion. Insular/trabecular/solid architecture was seen in all tumors; tumor necrosis was present in 23; median mitotic count was 6/2 mm^2, with a median Ki-67 proliferation index of 7.2%. Five patients had metastatic disease at presentation, with additional metastases in 3 patients; 18 were alive without evidence of disease (mean, 32.6 months); with the remaining 6 patients alive (n=2) or dead (n=4) with metastatic disease (mean, 20.1 months); overall median follow-up 27.7 months.

Criteria	Differentiated High Grade Follicular-cell Derived Thyroid Carcinoma (n = 17)	Poorly Differentiated Thyroid Carcinoma (n = 24)
Sex: Female / Male	9 / 8	13 / 11
Median age (mean), in years Females Males	64 (62) 57 (62) 65 (62)	58 (56) 50 (50) 66 (64)
Tumor size in cm, median (mean) (mean)	5.4 (5.8)	6.9 (6.5)
Tumor focality: Single Multifocal (i.e., other tumors present)	14 3	12 12
Tumor necrosis present	17 (all)	23 (96%)
Mitoses per 2 mm^2, median (mean)	5 (6.1)	6 (11)
Cells per mm^2 (median)	3379	4949
Ki-67 labelling index per mm^2 (median)	8.2%	7.2%
Extrathyroidal extension	4 (24%)	9 (38%)
Metastases at presentation	3 (17.6%)	5 (20.8%)
Additional metastases during follow-up	5 (29.4%)	3 (12.5%)
Follow-up (median in months): Alive, no evidence of disease Alive, with metastatic disease Dead, with no evidence of disease Dead, with metastatic disease	17 (23.9) 10 (19.7) 4 (25.8) None 3 (24.8)	24 (27.7) 17 (34.0) 2 (7.3) 1 (4.7) 4 (28.0)

Conclusions: DHGTC present at an older age without a sex predilection, showing tumor necrosis and a median Ki-67 proliferation index of 8.2%, with a higher percentage of patients with metastatic disease overall. PDTC presents about a decade earlier, with large tumors, often in a background of multifocal tumors. Tumor necrosis is nearly always seen, with a similar proliferation index. The overall median follow-up is similar between the groups, but metastatic disease is more common in the DHGTC group.

369 Medullary Thyroid Carcinoma Grading: An Interobserver Reproducibility Study

Jessica Williams[1], Melissa Zhao[1], Fedaa Najdawi[2], Sara Ahmadi[1], Jason Hornick[2], Kristine Wong[1], Justine Barletta[2]
[1]Brigham and Women's Hospital, Boston, MA, [2]Brigham and Women's Hospital, Harvard Medical School, Boston, MA

Disclosures: Jessica Williams: None; Melissa Zhao: None; Fedaa Najdawi: None; Sara Ahmadi: None; Jason Hornick: *Consultant*, Aadi Biosciences; *Consultant*, TRACON Pharmaceuticals; Kristine Wong: None; Justine Barletta: None

Background: Grade, based on proliferative rate and necrosis, has recently been shown to be prognostic in medullary thyroid carcinoma (MTC). The aim of this study was to evaluate the interobserver reproducibility of assessed grade in MTC.

Design: Three groups (each group included one resident and one attending pathologist) independently evaluated a cohort of sporadic MTC. For each case, all available tumor slides were reviewed, and mitotic count and the presence of tumor necrosis was recorded. Ki67 was performed, and the Ki67 proliferative index was determined in the area of highest proliferative activity (500-

2000 cells counted). Tumors were graded according to previously published Memorial Sloan Kettering (MSK) and Sydney grading systems (see Tables). Kappa statistics were calculated for each individual criterion (mitotic count, Ki67 proliferative index, and necrosis) and for assigned MSK and Sydney grade. The prognostic significance of grade was also determined based on recorded clinical outcome data.

Table 1: MSK Grading Scheme

Grade	Mitotic Count per 10 HPF	Coagulative Necrosis
Low	<5	Absent
High	<5	Present
High	≥5	Present or absent

Table 2: Sydney Grading Scheme

Grade	Mitotic Count per 10 HPF	Ki67 Proliferative Index (%)	Coagulative Necrosis
Low	<3	<3	Absent
Intermediate	<3	<3	Present
Intermediate	3-20	3-20	Absent
High	3-20	3-20	Present
High	>20	>20	Present or absent

Results: For our cohort of 44 MTC, the kappa statistic for mitotic count, Ki67 proliferative index, and necrosis was 0.54, 0.64, 0.89, respectively. The kappa statistic for assigned MSK grade was 0.84 and for assigned Sydney grade was 0.70. MSK and Sydney grade as assigned by each group was prognostic for progression-free survival and disease-specific survival on univariate analysis.

Conclusions: There was substantial interobserver agreement for assessment of grade in our cohort of MTC, indicating that MTC grade is not only prognostic, but also reproducible.

370 Germline CTNNA1 Pathogenic Variant Associated with Multiple Adenomas and Adenomatous Nodules with Intact PTEN Expression

Kristine Wong[1], Fei Dong[1], Huma Rana[2], Laura Goguen[1], Jason Hornick[3], Justine Barletta[3]
[1]Brigham and Women's Hospital, Boston, MA, [2]Dana-Farber Cancer Institute, Boston, MA, [3]Brigham and Women's Hospital, Harvard Medical School, Boston, MA

Disclosures: Kristine Wong: None; Fei Dong: None; Huma Rana: *Grant or Research Support*, Ambry Genetics Corporation, Invitae Corporation; Laura Goguen: None; Jason Hornick: *Consultant*, Aadi Biosciences, TRACON Pharmaceuticals; Justine Barletta: None

Background: The finding of multiple adenomas and adenomatous nodules in the thyroid is not specific but can be associated with the *PTEN*-associated tumor syndrome, Cowden syndrome (CS). However, in some cases that appear histologically identical to CS, PTEN expression is intact by immunohistochemistry (IHC), and clinical stigmata of CS are lacking. Germline *CTNNA1* (alpha-E-catenin) pathogenic variants have been associated with hereditary diffuse gastric cancer that lacks germline *CDH1* variants.

Design: We identified 2 patients with thyroidectomy findings similar to those seen in CS who had germline *CTNNA1* variants. We describe the clinical features, histologic findings, and associated gastric pathology.

Results: Case 1, a 42-year-old woman with a history of gastric bypass and family history of breast, thyroid, renal, and ovarian carcinoma, presented with multinodular goiter. She underwent hemithyroidectomy after indeterminate fine needle aspiration diagnoses of 2 nodules. The 48-gram hemithyroidectomy had numerous non-invasive, variably encapsulated nodules (up to 3.5 cm) with a solid/nested growth pattern and minimal cytologic atypia, no necrosis, and a low mitotic count. IHC for PTEN showed intact expression within the nodules. Next-generation sequencing performed on 2 nodules demonstrated that both had 2 loss of function variants in *CTNNA1*: both shared a *CTNNA1* p.R731* variant and had different second variants (*CTNNA1* p.C772* and *CTNNA1* p.D200Mfs*44). Subsequent germline testing confirmed the *CTNNA1* p.R731* variant. The patient underwent a completion thyroidectomy (with similar findings) and a risk-reducing (RR) gastrectomy, which revealed a 1.0 cm poorly differentiated adenocarcinoma with signet-ring-cell and neuroendocrine features (pT1a N0). Case 2, father of Case 1, shared the *CTNNA1* p.R731* germline variant. This 68-year-old man with no oncologic history was found to have multiple bilateral nodules on thyroid ultrasound. He underwent thyroidectomy which showed multiple adenomas and adenomatous nodules. A RR gastrectomy was negative for tumor.

Conclusions: To our knowledge, this is the first reported association of germline *CTNNA1* pathogenic variants with multiple adenomas and adenomatous nodules of the thyroid. Recognition of CS-like thyroid pathology may facilitate identification of germline cancer predisposition syndromes other than CS.

371 Redefining Solid Variant of Papillary Thyroid Carcinoma (PTC-SV): A Multicentric Retrospective Study

Bin Xu[1], Liz Edmund[2], Lingxin Zhang[3], Olivia Ganly[1], Kartik Viswanathan[4], Daniel Lubin[5], Ronald Ghossein[1]
[1]Memorial Sloan Kettering Cancer Center, New York, NY, [2]The University of Texas MD Anderson Cancer Center, Houston, TX, [3]Mount Sinai Hospital, University of Toronto, Toronto, Canada, [4]Emory University, Atlanta, GA, [5]Emory University Hospital, Atlanta, GA

Disclosures: Bin Xu: None; Liz Edmund: None; Lingxin Zhang: None; Olivia Ganly: None; Kartik Viswanathan: None; Daniel Lubin: None; Ronald Ghossein: None

Background: PTC-SV is considered as an aggressive variant. However, the definition of PTC-SV varies from >50% to nearly 100% of solid/trabecular/insular growth (STI). Furthermore, the presence of ≥30% STI precludes a diagnosis of noninvasive follicular thyroid neoplasm with papillary-like nuclear features (NIFTP). In this multicentric retrospective study, we aimed to establish an appropriate STI cutoff to define PTC-SV and identify prognostic factors in PTC with STI.

Design: 120 PTCs with various proportion of STI were included. The primary outcomes were risk of nodal metastasis and recurrence free survival (RFS). For multifocal tumors, only those with the largest tumor containing STI were included.

Results: The risk of nodal metastasis significantly correlated with encapsulation/infiltration ($p<0.001$) but not the percentage of STI ($p=0.781$). N1 disease was seen in 1-3% of encapsulated and 43-59% of infiltrative PTC regardless of STI percentage (Figure). Other parameters associated with nodal metastasis were percentage of papillary and follicular architecture, vascular invasion, margin status, extrathyroidal extension (ETE) and AJCC pT stage. Six patients developed distant metastasis whereas 2 had locoregional recurrence. The 10-year DFS was 89% in the entire cohort, 98% in encapsulated lesions, and 75% in infiltrative tumors. STI percentage did not impact DFS ($p=0.239$). Other significant prognostic factors included vascular invasion, histologic and gross ETE, AJCC pT and pN stage and tumor size. 50 patients had noninvasive encapsulated lesion with 2% to 100% STI. Among them 35 did not meet NIFTP criteria given the presence of papillae (n=3), ≥30% STI (n=29), or 3-4 mitoses/10 high power fields (n=3). One patient with a 2.7cm tumor composed of 80% STI and 4 additional papillary microcarcinomas classic type had psammoma bodies within the central compartment lymph nodes. None developed recurrence. Lastly, we studied the status of RAS mutations and BRAF V600E mutations in a subset of 76 patients. Encapsulated lesions were enriched with RAS mutations (54%), whereas infiltrative lesions lacked RAS mutations (4%). BRAF V600E mutation was an infrequent event, being seen in 11% of the entire cohort, 8% of encapsulated and 17% of the infiltrative lesions.

Figure 1 - 371

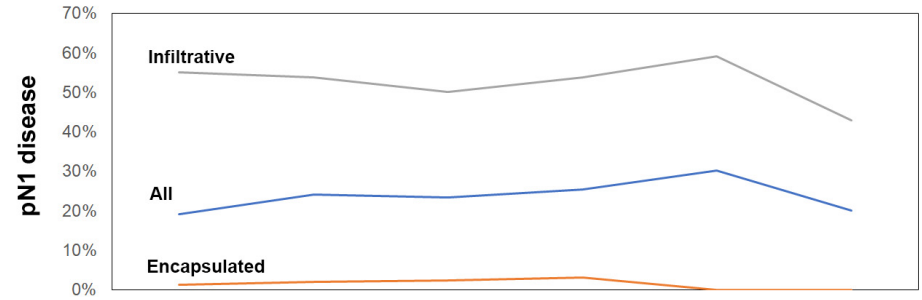

STI%	≥1%	≥30%	≥50%	≥70%	≥90%	100%
All cases	23/120 (19%)	22/91 (24%)	18/77 (24%)	15/59 (25%)	13/43 (30%)	3/15 (20%)
Encapsulated	1/80 (1%)	1/52 (2%)	1/43 (2%)	1/33 (3%)	0/21 (0%)	9/8 (0%)
Infiltrative	22/40 (55%)	21/39 (54%)	17/34 (50%)	14/26 (54%)	13/22 (59%)	3/7 (43%)

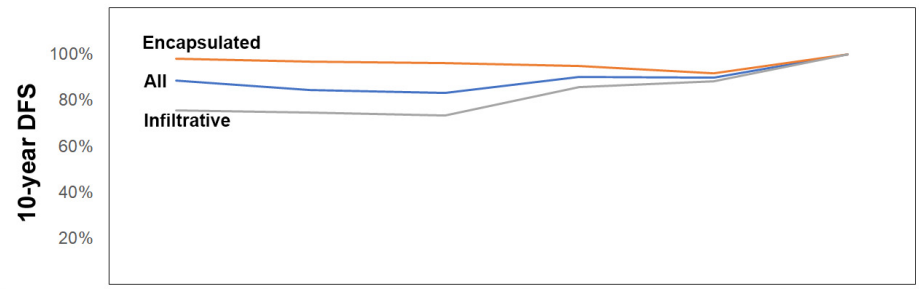

STI%	≥1%	≥30%	≥50%	≥70%	≥90%	100%
All cases	89%	84%	83%	90%	90%	100%
Encapsulated	98%	97%	96%	95%	92%	100%
Infiltrative	75%	75%	73%	86%	88%	100%

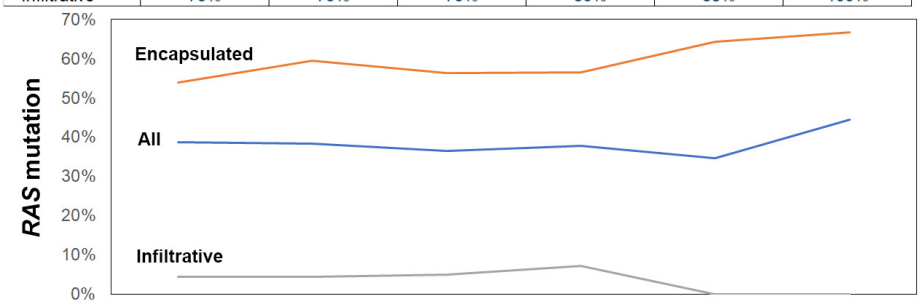

STI%	≥1%	≥30%	≥50%	≥70%	≥90%	100%
All	29/75 (39%)	23/60 (38%)	19/52 (37%)	14/37 (38%)	9/26 (35%)	4/9 (44%)
Encapsulated	28/52 (54%)	22/37 (59%)	18/32 (56%)	13/23 (57%)	9/14 (64%)	4/6 (67%)
Infiltrative	1/23 (4%)	1/23 (4%)	1/20 (5%)	1/14 (7%)	0/12 (0%)	0/3 (0%)

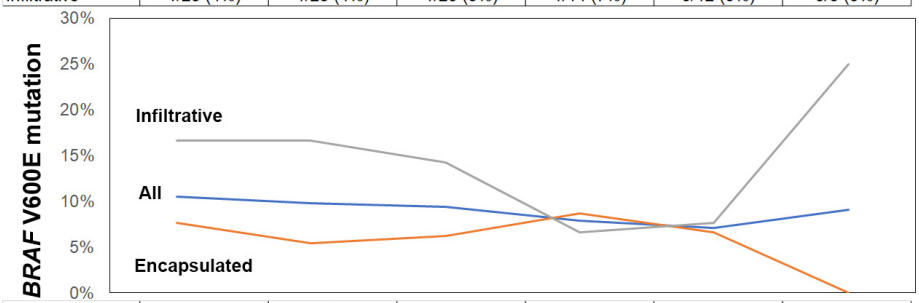

STI%	≥1%	≥30%	≥50%	≥70%	≥90%	100%
All	8/76 (11%)	6/61 (10%)	5/53 (9%)	3/38 (8%)	2/28 (7%)	1/11 (9%)
Encapsulated	4/52 (8%)	2/37 (5%)	2/32 (6%)	2/23 (9%)	1/15 (7%)	0/7 (0%)
Infiltrative	4/24 (17%)	4/24 (17%)	3/21 (14%)	1/15 (7%)	1/13 (8%)	1/4 (25%)

Conclusions: In PTC with STI, the determining factor for nodal metastasis and DFS is the encapsulation/infiltration status rather than STI percentage. Encapsulated noninvasive tumors with STI follow an indolent course with a very low risk of nodal metastasis and recurrence. Overall PTC with STI has an excellent prognosis with a 10-year DFS of 89%. Therefore, the classification of SV-PTC as an aggressive PTC subtype may be reconsidered in order to spare these patients unnecessary aggressive therapy. Further studies are needed to reassess the 30% STI threshold used to exclude NIFTP.